Experimentally accessible reentrant phase transitions in double-well optical lattices

Ippei Danshita[1,2], Carlos A. R. Sá de Melo[1,3], and Charles W. Clark[1]
[1] *Joint Quantum Institute, National Institute of Standards and Technology, and University of Maryland, Gaithersburg, Maryland 20899, USA*
[2] *Department of Physics, Waseda University, Shinjuku-ku, Tokyo 169-8555, Japan*
[3] *School of Physics, Georgia Institute of Technology, Atlanta, Georgia 30332, USA*
(Dated: February 2, 2008)

We study the quantum phases of bosons confined in a combined potential of a one-dimensional double-well optical lattice and a parabolic trap. We apply the time-evolving block decimation method to the corresponding two-legged Bose-Hubbard model. In the absence of a parabolic trap, the system of bosons in the double-well optical lattice exhibits a reentrant quantum phase transition between Mott insulator and superfluid phases at unit filling as the tilt of the double-wells is increased. We show that the reentrant phase transition occurs also in the presence of a parabolic trap and suggest that it can be detected in experiments by measuring the matter-wave interference pattern.

PACS numbers: 03.75.Hh, 03.75.Lm, 05.30.Jp

Recently, the system of ultracold bosonic atoms in a double-well optical lattice (DWOL) has been used to study quantum information processing and quantum many-body systems [1, 2, 3, 4]. A DWOL is constructed from two-color two-dimensional (2D) lattices in the horizontal xy plane and another lattice in the vertical z direction, resulting in a 3D lattice whose unit cell is a double well. By exploiting precise control of the properties of the double wells, recent experiments have realized an atom interferometer [2], two-atom exchange oscillations, which were used to create a quantum SWAP gate [3], and correlated tunneling of two interacting atoms [4].

In single-well optical lattices, the transition from a superfluid (SF) phase to a Mott insulator (MI) phase has been observed by adiabatically increasing the lattice depth [5, 6]. In previous DWOL experiments all the double wells were independent of each other due to the large potential barrier between them, and the system was always in an insulating phase. However, the potential barrier could be lowered to induce a transition to a SF phase [1]. In particular, one can investigate the SF-MI transition in a two-legged ladder 1D DWOL by tuning the lattice depth in the vertical direction. While in single-well lattices the SF-MI transition is determined by the ratio, U/t, of the on-site interaction energy to the hopping energy [5, 6], in DWOL the SF-MI transition is governed by the competition between the on-site interaction and the tilt (energy offset) of the double wells.

In this paper, we study the ground state properties of bosons in a two-legged ladder lattice with a parabolic confining potential. This case is more representative of current experiments than is an unconfined, homogeneous lattice. Although mean-field-type methods describe the SF-MI transition of bosons in optical lattices very well in 3D [7], they fail to describe quantitatively the two-legged ladder system due to strong quantum fluctuations [8]. Hence, we use the time-evolving block decimation (TEBD) method [9, 10], which is one of the best methods currently available to study strongly correlated 1D quantum systems. We show here that a reentrant phase transition (MI-SF-MI) occurs as the tilt of the double wells is changed for a fixed parabolic confinement. Moreover, a distinctive signature of the reentrant phase transition appears in the momentum distribution, which is directly related to matter-wave interference patterns observed in experiments.

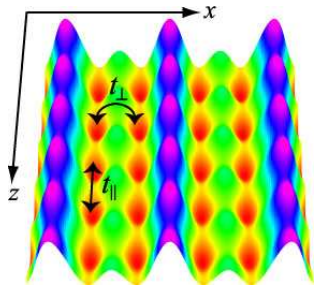

FIG. 1: (color online) Schematic double-well lattice potential in the xz plane for $\alpha = 0.2$, $\theta = 0$, showing the existence of isolated two-legged ladders.

We consider a Bose gas at zero temperature confined in a combined potential of a DWOL and a parabolic trap. A DWOL potential in Refs. [1, 2, 3] is given by

$$V(\boldsymbol{r}) = V_{\rm in}\left(\sin^2(kx) + \sin^2(ky) - 2\right) - V_{\rm out}\left(\sin(kx-\theta) + \cos(ky)\right)^2 + V_{\rm z}\sin^2(kz), \quad (1)$$

where $V_{\rm in}$ is the depth of the "in-plane" lattice with period of $d \equiv \pi/k$, whose light polarization is in the xy plane, $V_{\rm out}$ the depth of the "out-of-plane" lattice with $2d$-periodicity [1], and $V_{\rm z}$ is the depth of the lattice in the vertical z direction. When the ratio $\alpha \equiv V_{\rm out}/V_{\rm in}$ satisfies $0 < \alpha < 0.5$, the unit cell of the potential Eq. (1) is a double-well. Control of the ratio α and the relative phase θ provides the flexibility to adjust the double-well parameters: the barrier height and the tilt. When $\theta = 0$, the double wells are symmetric (no tilt). Increasing α from zero enlarges the barrier height $V_{\rm high}$ between double wells in the xy plane and reduces the barrier height $V_{\rm low}$ between two wells within a double well. Keeping

$V_{\rm high} - V_{\rm low} \gg E_{\rm R}$ and tuning $V_{\rm z}$, one can create an ensemble of 1D DWOLs with a two-legged ladder structure, where all the two-legged ladders are decoupled from each other as shown in Fig. 1. Here $E_{\rm R} = \frac{\hbar^2 k^2}{2m}$ is the recoil energy, where m is the boson mass.

At zero temperature the many-body quantum state of interacting bosons in an optical lattice is well described by the Bose-Hubbard model when the lattice is so deep that only the lowest energy level of each lattice site is occupied and tunneling occurs only between nearest-neighboring sites [11, 12]. To study bosons in 1D DWOLs, we use the two-legged Bose-Hubbard Hamiltonian (BHH)

$$H = \sum_j \Big\{ \sum_{\eta\in\{L,R\}} \Big(\frac{U}{2}\hat{n}_{j,\eta}(\hat{n}_{j,\eta}-1) + (\Omega j^2 - \mu)\hat{n}_{j,\eta} - t_{\parallel}(a^\dagger_{j+1,\eta}a_{j,\eta} + \text{h.c.}) \Big) - t_\perp (a^\dagger_{j,R}a_{j,L} + \text{h.c.}) + \frac{\lambda}{2}(\hat{n}_{j,L} - \hat{n}_{j,R}) \Big\}. \quad (2)$$

$a^\dagger_{j,\eta}$ creates a boson at the lowest level localized on the left (right) of the j-th double-well for $\eta = L(R)$, and $\hat{n}_{j,\eta} = a^\dagger_{j,\eta}a_{j,\eta}$ is the number operator. The lattice parameters can be related to the DWOL depths $V_{\rm in}$, $V_{\rm out}$, and V_z and the recoil energy $E_{\rm R}$ by assuming that $\theta \ll 1$ and that each well is sufficiently deep to approximate the Wannier function by a Gaussian. In this case, the on-site interaction is $U \sim E_{\rm R}(8\pi)^{1/2}\frac{a_{\rm s}(1-2\alpha)^{1/4}}{d(1-\alpha)^{1/2}} s_{\rm z}^{1/4} s^{1/2}$; the intrachain hopping is $t_{\parallel} \sim E_{\rm R}\left(\frac{\pi^2}{4}-1\right) s_{\rm z}\, e^{-\pi^2\sqrt{s_{\rm z}}/4}$; the interchain hopping is $t_\perp \sim E_{\rm R}\left(\sqrt{\frac{1-2\alpha}{1-\alpha}}f(\alpha) - 1 + 2\alpha\right) s\, e^{-f(\alpha)\sqrt{s}}$; the tilt (energy offset) of the double wells is $\lambda \sim E_{\rm R}\frac{4\alpha\sqrt{1-2\alpha}}{(1-\alpha)^2} s\theta$. Here, $\alpha = V_{\rm out}/V_{\rm in}$, $s = V_{\rm in}/E_{\rm R}$, $s_{\rm z} = V_{\rm z}/E_{\rm R}$, $a_{\rm s}$ is the s-wave scattering length, and $f(\alpha) = \sqrt{\frac{1-2\alpha}{1-\alpha}}\arccos^2\left(\frac{\alpha}{1-\alpha}\right)$. Ω is the curvature of the parabolic trap, and μ is the chemical potential, which controls the total number of bosons N. Notice that U, $t_{\parallel}$, and $t_\perp$ are approximately independent of the tilt as long as $\theta \ll 1$.

We now describe briefly the zero-temperature phase diagrams of the two-legged Bose-Hubbard model with no confining potential ($\Omega = 0$) [8, 13, 14]. In Figs. 2(a)-(c), we show the phase diagrams in the $(\mu/U, t_{\parallel}/U)$ plane for $t_\perp/U = 0.1$. There we see the usual MI phase with unit filling, $\nu = 1$ (corresponding to two atoms per double well), and also one with half filling, $\nu = 1/2$ [8, 13]. The SF-MI phase boundary in the $(\mu/U, t_{\parallel}/U)$ plane significantly depends on $t_\perp/U$ [14] and λ/U [8]. In particular, the unit-filling MI phase depends nonmonotonically upon λ/U. As seen in the upper lobes of the phase diagrams, the $\nu = 1$ MI region shrinks initially as λ/U is increased from zero. The size of the MI region is minimized at $\lambda = U$, where the local states $|1,1\rangle$ and $|0,2\rangle$ are nearly degenerate; $|n_L, n_R\rangle$ designates the local Fock state with $n_L(n_R)$ bosons on the left (right) of a double well. Due to this degeneracy, coherence is developed within each double well and the system favors the SF phase. As λ/U is increased further, the MI region grows again. This nonmonotonic behavior leads to a reentrant phase transition from a MI to a SF and again to a MI, induced by increasing λ/U.

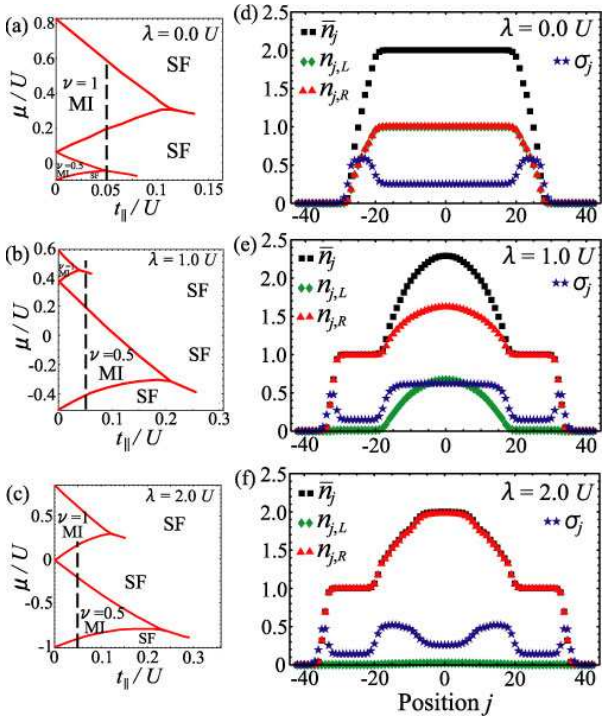

FIG. 2: (color online) Results at three values of λ/U: 0 (a) and (d), 1 (b) and (e), and 2 (c) and (f). In the left three figures, we show the phase diagrams of the homogeneous system in the $(\mu/U, t_{\parallel}/U)$ plane for $t_\perp = 0.1U$, which have been calculated by means of the infinite-size version of the TEBD method. In the right three figures, the local number of bosons at the j-th double-well $\bar{n}_j$ (squares), that at the j-th left well (diamonds), that at the j-th right well (triangles), and the fluctuation σ_j of $\bar{n}_j$ (stars) are shown. The dashed lines in the phase diagrams represent the values of the local chemical potential and the intrachain hopping realized in the right figures. The upper (lower) end of the dashed lines corresponds to the center (edges) of the trapped gas.

Since we are mainly interested in the reentrant phase transition, we investigate how the ground state properties change with increasing λ/U for the following fixed values of the other parameters; $N = 98$, $\Omega/U = 0.001$, $t_\perp/U = 0.1$, and $t_{\parallel}/U = 0.05$. This value of $t_{\parallel}/U$ is sufficiently small such that the MI domain with $\nu = 1$ is present when $\lambda = 0$ or $\lambda \gg U$, while it is so large that the $\nu = 1$ MI domain is absent when $\lambda = U$. The number of double wells is chosen as $L = 85$. This value of L is so large that the bosons do not see the edge of the system.

To analyze the two-legged BHH (2), we use the finite-size version of the TEBD method [9], which provides a precise ground state for 1D quantum lattice systems via propagation in imaginary time. While the maximum

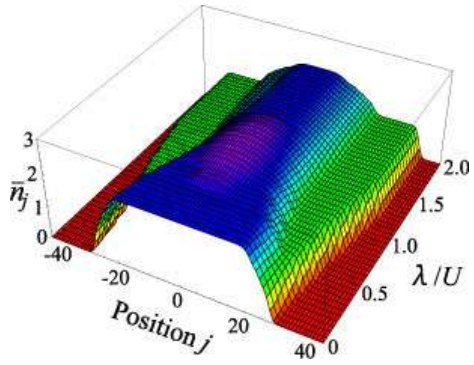

FIG. 3: (color online) Density profile $\bar{n}_j$ as a function of λ/U. All the other parameters are fixed as $N = 98$, $L = 85$, $t_\parallel/U = 0.05$, $t_\perp/U = 0.1$, and $\Omega/U = 0.001$.

number of bosons per site is $N_{\max} = \infty$, convergence is already achieved in our numerical calculations when $N_{\max} = 5$. We calculate the ground states of the Hamiltonian (2) with $\chi = 80$, where χ is the size of the basis set retained in the TEBD procedure [9].

In Fig. 3, we show the density profile $\bar{n}_j = n_{j,L} + n_{j,R} = \sum_\eta \langle \hat{n}_{j,\eta} \rangle$, namely the local number of bosons in the j-th double well as a function of λ/U. For $\lambda = 0$, the system is essentially a plateau with unit filling ($\bar{n}_j = 2$), with small SF regions with incommensurate filling at the edges. This plateau indicates the presence of an incompressible MI domain [6, 15, 16, 17, 18]. As λ/U is increased, the unit-filling plateau starts to melt at a certain point and a new MI plateau with half filling ($\bar{n}_j = 1$) emerges. In the vicinity of $\lambda = U$, the unit-filling plateau has been completely melted away and the density profile for $\bar{n}_j > 1$ is smooth, with the reflected parabolic shape of the confining potential that is characteristic of SF phases in the regime where the local density approximation is valid [15]. As λ/U is increased further, the unit-filling plateau forms again at the center of the system. Thus, as in the homogeneous case, the reentrant phase transition is caused by increasing the tilt parameter in the presence of a parabolic potential [19].

For a better understanding of the reentrant phase transition, three slices from Fig. 3 are shown in Figs. 2(d)-(f) together with $n_{j,L}$, $n_{j,R}$, and the fluctuation of $\bar{n}_j$, $\sigma_j = \sqrt{\langle \hat{n}_j^2 \rangle - \bar{n}_j^2}$, which is small in the MI regions and relatively large in the SF regions. One can roughly interpret the spatial dependence of $\bar{n}_j$ by a local density approximation. Introducing the effective local chemical potential $\mu_j^{\rm eff} = \mu - \Omega j^2$, $\bar{n}_j$ is approximated by $\tilde{n}(\mu_j^{\rm eff})$, where $\tilde{n}(\mu)$ is the number of bosons per double well for uniform systems. Scanning the effective chemical potential along the dashed lines in the phase diagrams of Figs. 2(a)-(c), the behavior of the local density in Figs. 2(d)-(f) can be explained. When $\lambda = U$, for example, the upper end of the dashed line in Figs. 2(b) is located in a SF phase with $\tilde{n} > 2$ as realized at the center of the trapped gas in Fig. 2(e). As μ is decreased from

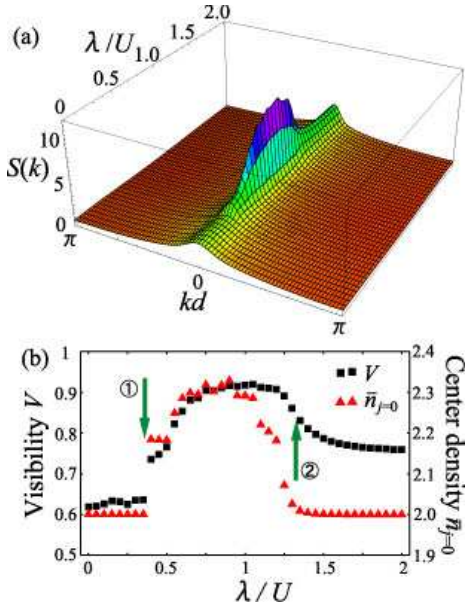

FIG. 4: (color online) (a) Quasi-momentum distribution $S(k)$ as a function of λ/U. (b) Visibility V (squares) and center density $\bar{n}_{j=0}$ (triangles) as functions of λ/U.

the upper end, the dashed line enters the MI phase with half filling, corresponding to the half-filling plateau of the trapped gas. As μ is decreased further to the lower end, the dashed line exits to a SF phase with $\tilde{n} < 1$, which is also realized at the boundary of the trapped gas. Notice that the local density approximation breaks down in the vicinity of the interfaces between the commensurate and incommensurate regions, where the singularities due to quantum critical behavior observed in uniform systems are removed [16, 17].

In Figs. 2(d)-(f), the population of bosons in the left wells shifts gradually to the right wells as λ/U is increased. At $\lambda = U$, almost all the bosons occupy the right wells, namely $n_{j,L} \simeq 0$, for $\bar{n}_j \leq 1$. In contrast, a considerable amount of bosons remains in the left well as $n_{j,L} \simeq \frac{\bar{n}_j - 1}{2}$ for $\bar{n}_j > 1$, since the local state with unit-filling is approximately given by $(|1,1\rangle + |0,2\rangle)/\sqrt{2}$ due to the competition between the onsite interaction and the tilt. At $\lambda = 2U$, the population of bosons in the left well almost vanishes, namely $n_{j,L} \simeq 0$, in the entire system.

Next, we calculate the quasi-momentum distribution $S(k) = L^{-1} \sum_{j,l} \sum_\eta e^{ik(j-l)d} \langle a_{j,\eta}^\dagger a_{l,\eta} \rangle$, where d is the lattice spacing. Since the true-momentum distribution is expressed as the product of $|w(k)|^2$ and $S(k)$ [18], where $w(k)$ is the Fourier transform of the Wannier function in the lowest Bloch band, the quasi-momentum distribution can be extracted by dividing the true-momentum distribution observed in experiments by $|w(k)|^2$ [6]. $S(k)$ is shown as a function of λ/U in Fig. 4(a), where the $k = 0$ peak is the sharpest in the vicinity of $\lambda = U$. This means the intrachain coherence increases as the SF region around the trap center emerges.

To quantify the sharpness of the peak in $S(k)$, we cal-

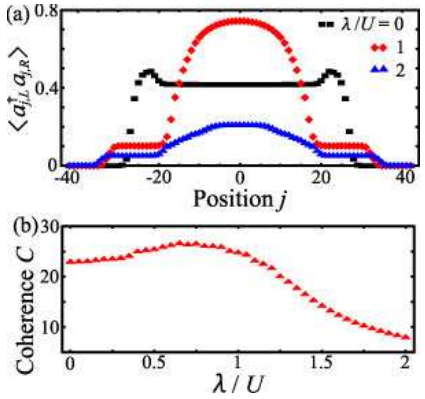

FIG. 5: (color online) (a) Local coherence between the left and right wells $\langle a^\dagger_{j,L} a_{j,R} \rangle$ for $\lambda/U = 0$ (squares), 1 (diamonds), and 2 (triangles). (b) Total coherence C versus λ/U.

culate the visibility of interference patterns defined as $V = (S_{\max} - S_{\min})/(S_{\max} + S_{\min})$ [20, 21]. In Fig. 4(b), we show V and the center density $\bar{n}_{j=0}$ as a function of λ/U. As indicated by the first arrow, the visibility exhibits a sudden jump at the point where the unit-filling MI plateau starts to melt. In the vicinity of $\lambda = U$, where the unit-filling MI plateau does not exist, the visibility is distinctively large compared to the regions where the unit-filling MI plateau is present. As λ/U is increased further, the visibility decreases the most rapidly at the point indicated by the second arrow, where the $\nu = 1$ MI plateau forms again. Notice that the change of the visibility at the second arrow is not as distinctive as the jump at the first arrow because the $\nu = 1$ Mott plateau at $\lambda = 2U$ is small compared to that at $\lambda = 0$. This tendency of the visibility suggests that the reentrant phase transition can be characterized in experiments through the observation of matter-wave interference patterns.

Another key observable in DWOLs is the coherence between the left and right wells $C = \sum_j \langle a^\dagger_{j,L} a_{j,R} \rangle$. The coherence C can be extracted from the double-slit diffraction pattern, which has been observed in the time-of-flight images in the horizontal xy plane [1, 2, 3]. The larger C is, the clearer the diffraction pattern is.

We calculate first the local coherence $\langle a^\dagger_{j,L} a_{j,R} \rangle$ as shown in Fig. 5(a). At $\lambda = 0$, since the local state with half-filling is well approximated by the bonding state, the SF regions at the boundary of the trapped gas have large local coherence. As λ/U is increased, the region with $\bar{n}_j \leq 1$ immediately loses the local coherence. In contrast, in the region with $\bar{n}_j > 1$ the local coherence is pronouncedly large at $\lambda = U$. The development of local coherence is due to the degeneracy of $|1, 1\rangle$ and $|0, 2\rangle$ states, and it drives the system into the SF phase. As λ/U is increased further, the entire system tends to lose coherence. In Fig. 5(b), the total coherence C is shown as a function of λ/U. While the total coherence is significantly reduced when λ is increased from U, it hardly changes in the region $\lambda < U$. This happens because the gain of local coherence for $\bar{n}_j > 1$ and the loss for $\bar{n}_j \leq 1$ almost cancel each other out. Consequently, the double-slit diffraction pattern can not capture the signature of the reentrant phase transition.

In conclusion, we have studied the SF-MI transition of parabolically trapped Bose gases in a 1D double-well optical lattice by using the time-evolving block decimation (TEBD) method. We have calculated the density profile as a function of the tilt of the double wells and shown that a reentrant phase transition between MI and SF phases occurs in the presence of a parabolic confinement. We have calculated also the quasi-momentum distribution and found that the matter-wave interference pattern, which is one of the most common observables in experiments with cold atoms, contains sufficient information to characterize the reentrant phase transition. We would like to emphasize that, unlike the results of mean-field theories, our results based on the TEBD method are quantitative, thus we expect the reentrant phase transition to be observed in future experiments near the parameter values discussed in this paper.

We thank Jamie Williams and Trey Porto for stimulating discussions. I. D. also thanks Gabriele De Chiara for helpful discussions regarding the TEBD algorithm. I. D. acknowledges support from a Grant-in-Aid from JSPS, and C. SdM thanks NSF (DMR - 0709584) for support.

[1] J. Sebby-Strabley *et al.*, Phys. Rev. A **73**, 033605 (2006).
[2] J. Sebby-Strabley *et al.*, Phys. Rev. Lett. **98**, 200405 (2007).
[3] M. Anderlini *et al.*, Nature (London) **448**, 452 (2007).
[4] S. Fölling *et al.*, Nature (London) **448**, 1029 (2007).
[5] M. Greiner *et al.*, Nature (London) **415**, 39 (2002).
[6] I. B. Spielman *et al.*, Phys. Rev. Lett. **98**, 080404 (2007).
[7] D. van Oosten *et al.*, Phys. Rev. A **63**, 053601 (2001).
[8] I. Danshita *et al.*, Phys. Rev. A **76**, 043606 (2007).
[9] G. Vidal, Phys. Rev. Lett. **93**, 040502 (2004).
[10] G. Vidal, Phys. Rev. Lett. **98**, 070201 (2007).
[11] M. P. A. Fisher *et al.*, Phys. Rev. B **40**, 546 (1989).
[12] D. Jaksch *et al.*, Phys. Rev. Lett. **81**, 3108 (1998).
[13] P. Buonsante *et al.*, Phys. Rev. A **72**, 031602(R) (2005).
[14] P. Donohue *et al.*, Phys. Rev. B **63**, 180508(R) (2001).
[15] C. Kollath *et al.*, Phys. Rev. A **69**, 031601(R) (2004).
[16] G. G. Batrouni *et al.*, Phys. Rev. Lett. **89**, 117203 (2002).
[17] S. Wessel *et al.*, Phys. Rev. A **70**, 053615 (2004).
[18] V. A. Kashurnikov *et al.*, Phys. Rev. A **66**, 031601(R) (2002).
[19] Strictly speaking, because of the lack of critical behavior, the transition between MI and SF phases in parabolically confined systems is not a true quantum phase transition [16, 17].
[20] F. Gerbier *et al.*, Phys. Rev. Lett. **95**, 050404 (2005).
[21] P. Sengupta *et al.*, Phys. Rev. Lett. **95**, 220402 (2005).